Biomolecular Electronic Devices Based on Self-Organized Deoxyguanosine Nanocrystals

ROSS RINALDI,[a] EMANUELA BRANCA,[a] ROBERTO CINGOLANI,[a] ROSA DI FELICE,[b] ARRIGO CALZOLARI,[b] ELISA MOLINARI,[b] SALVATORE MASIERO,[c] GIANPIERO SPADA,[c] GIOVANNI GOTTARELLI,[c] AND ANNA GARBESI[d]

[a]*National Nanotechnology Laboratory (NNL), Istituto Nazionale per la Fisica della Materia (INFM) and Dipartimento di Ingegneria dell'Innovazione, Università di Lecce, Via Arnesano, 73100 Lecce, Italy*

[b]*Istituto Nazionale per la Fisica della Materia (INFM) and Dipartimento di Fisica, Università di Modena e Reggio Emilia, Via Campi 213a, 41100 Modena, Italy*

[c]*Dipartimento di Chimica Organica "A. Mangini," Università di Bologna, Viale del Risorgimento 4, 40136 Bologna, Italy*

[d]*ISOF, Area della Ricerca CNR, Via P. Gobetti 101, 40129 Bologna, Italy*

ABSTRACT: We report on a new class of hybrid electronic devices based on a DNA nucleoside (deoxyguanosine lipophilic derivative) whose assembled polymeric ribbons interconnect a submicron metallic gate. The device exhibits large conductivity at room temperature, rectifying behavior and strong curent–voltage hysteresis. The transport mechanism through the molecules is investigated by comparing films with different self-assembling morphology. We found that the main transport mechanism is connected to π–π interactions between guanosine molecules and to the formation of a strong dipole along ribbons, consistently with the results of our first-principles calculations.

KEYWORDS: molecular electronic; DNA nucleosides; self-assembly electronic devices; transport; nanotechnology

There is growing interest in the interconnection of biological molecules with inorganic materials (like metals and semiconductors), both for the implementation of novel functional devices and for ultimate electronic device miniaturization.[1–5] The combination of self-organization and recognition properties of biological matter with nanopatterning technologies provides a unique tool for the realization of new

Address for correspondence: Ross Rinaldi, Istituto Nazionale per la Fisica della Materia (INFM) and Dipartimento di Ingegneria dell'Innovazione, Università di Lecce, Via Arnesano, 73100, Italy. Voice: +39-0832-320238-326351; fax: +39-0832-326351.
ross.rinaldi@unile.it

Ann. N.Y. Acad. Sci. 960: 184–192 (2002).

hybrid molecular electronic devices. More specifically, there have been several attempts to measure and exploit the conductivity of DNA molecules bridging metallic patterns at the micro- and nano- scales.[6,7] Measurements of electrical transport through DNA molecules connecting two metallic electrodes have evidenced a rather controversial behavior of such molecules, showing either insulating or semiconducting properties depending on the specific experiments.[8–10] The basic mechanism of such electronic properties is not yet fully understood. In this paper we focus on the electronic properties of a modified DNA base, lipophilic deoxyguanosine derivative I, which exhibits strong self-assembly properties, resulting in the formation of two-dimensional ordered aggregates of ribbons in the solid state. The aggregates form a sort of biological nanocrystal showing a clear semiconductor behavior with blue band-gap and coherent band transport. These are used, in combination with nanopatterned metallic contacts separated by narrow gaps between 800 nm and 30 nm, to fabricate novel biomolecular electronic devices with excellent photodiode behavior and metal/semiconductor/metal characteristics at room temperature.

FIGURE 1a shows the deoxyguanosine molecule and the ribbonlike structure formed in the solid state, after a controlled evaporation of the solvent in a chloroform solution. The molecules were chosen because of their self-recognition and self-assembly properties.[11,12] The self-organization into a ribbonlike structure occurs spontaneously in solution and can be reproduced in the solid state upon well-controlled evaporation of the solvent. To this aim, different chloroform solutions were prepared and gently evaporated in a dry environment onto a nanometer-sized gap opened between two gold nanoelectrodes (FIG. 1b). The molar concentration for the formation of the biological nanocrystal (BNC) ranged between 0.01 M and 0.04 M. Concentrations outside this range resulted in totally disordered systems. The network formed by the guanosine derivative turned out to be very interesting in view of the singular electron donor properties of the base.[13] The gold nanocontacts were fabricated by electron beam lithography (EBL) on a SiO_2 substrate (of roughness below 0.2 nm). The gap size varied between 30 nm and 800 nm.

The self-organization of the solid-state molecular film in the gold nanogap was carefully checked by atomic force microscopy (AFM) measurements (FIG. 1c). The molecules formed an ordered lamellar structure where the ribbons extended over a length typically on the order of 100 nm. On this scale, the material has the properties of a nanocrystal formed by aligned deoxyguanosine molecules. At longer distances the orientation is lost, and randomly oriented clusters composed of oriented ribbons are formed, just like in polycrystalline materials. The ribbons in each BNC are closely packed and parallel; they are aligned randomly with respect to the contacts. The typical size of the ribbon is 2.4 nm in width (excluding the alkyl chains) and about 100 nm in length (l).

The gap width L between the gold electrodes was purposely varied within the range $30 < L < 120$ nm, in order to measure the current transport through a single BNC ($l < 100$ nm) and through the polycrystalline ensemble of BNCs ($L > 100$ nm). The current–voltage (I-V) characteristics of the biomolecular hybrid devices were measured at room temperature in the dark. The I-V curves are reported in FIGURE 2 and show a striking dependence on the length of the metal gap. For wide gaps ($L = 800$ nm), we find a symmetric nonohmic behavior and a clear hysteresis loop in the downward–upward sweeps (FIG. 2a). This is characteristic of a metal–dielectric–metal structure, where the presence of a thin potential barrier causes a symmetric

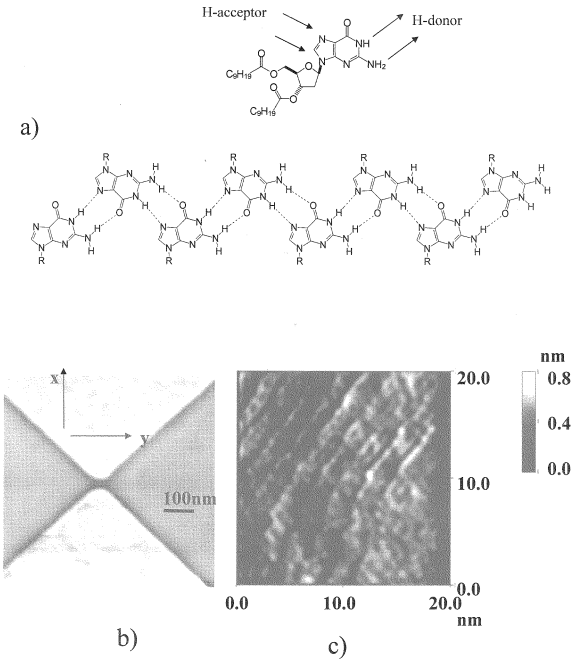

FIGURE 1. (a) 3′,5′-di-*O*-decanoyl-2′-deoxyguanosine (I) molecule and a typical ribbonlike aggregate of the molecule. The molecule was prepared following a modified procedure with respect to that described in Gottarelli *et al.*,[12] avoiding the use of inorganic salts and silica gel. A powder was obtained from anhydrous acetonitrile. **(b)** Scanning electron micrograph of the gold nanoelectrodes fabricated by EBL and lift-off onto a SiO_2/Si substrate. **(c)** AFM image of the molecular layer deposited in the gap between the two electrodes. One drop (3 μL) of a 0.03 M solution of deoxyguanosine in $CHCl_3$ was deposited in the gap between the electrodes. The AFM measurements were performed in contact mode and in air, after the slow evaporation of the solvent. A packed, ordered lamellar structure is clearly observed in the image and is consistent with the scanning, tunneling microscopy measurement performed on a similar deoxyguanosine crystalline structure in a liquid enviroment.[13] The supramolecular template consists of a closely packed array of hydrogen-bonded ribbons with interdigitated alkyl chains.

rectification of the *I-V* curves and the capacitance of the dielectric induces the hysteresis. This behavior is found to be reproducible in all wide-contact gaps ($L > 200$ nm), suggesting that the molecular film induces a capacitor effect in the planar device.

The situation changes dramatically in the 120-nm-wide gap device. In this case the length scale probed by the contacts is comparable to the self-ordering length l of the deoxyguanosine nanocrystal, and we expect that just a few clusters are probed by the electrodes. The *I-V* characteristics show a nonlinear symmetric behavior, with a zero current region in the voltage range between −2 V and +2 V. For bias higher than 2 V, the current increases to a sub-μA level, with a dynamical resistance of the

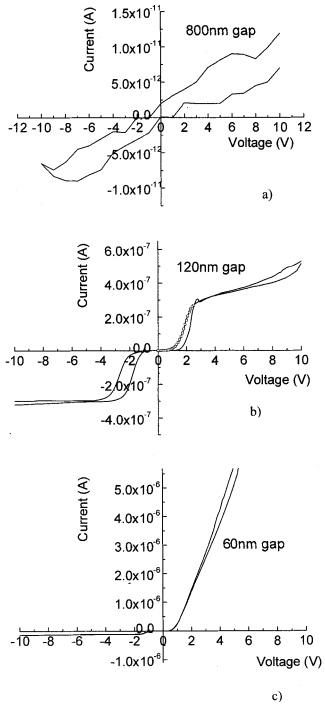

FIGURE 2. Current–voltage characteristics measured in three hybrid devices with gaps of 60, 120, and 800 nm between the electrodes. The measurements were performed at ambient pressure, in the dark, and with a humidity level of 54%. The noise level of the detector is in the fA range. All the realized electrodes were tested to give open-circuit current levels (noise level) before the molecular layer deposition. The *dotted line* on curve (b) is the simulation of the MSM characteristic performed by means of Eq. (1). The voltage was swept at 1 V/min.

order of a fraction of M, and then saturates. The shape of the *I-V* curve in this case is similar to that of the metal-semiconductor-metal (MSM) device. The device is a planar structure that can be schematized by two Schottky diodes connected in series back to back. The current flowing through the MSM device is given by:[14]

$$I = I_s e^{[-\beta(V - V_{fb})]/4V_{fb}} \quad \textbf{(1)}$$

where I_s is the saturation current, β is the ideality factor of the device, and V_{fb} is the flat band potential, corresponding to the voltage for which the electric field is zero at the right electrode. The simulation of our MSM device by Eq. (1) provides an excellent description of the *I-V* curve of FIGURE 2b (see dashed line), with a value of 7.49 V. Note that in this case the hysteresis is considerably reduced, as expected from the reduction of the capacity for the few BNCs probed in the gap and the consequent change in the conduction mechanism (see below). The MSM character of the device is further supported by the strong photoresponse under illumination (FIG. 3a). The response of the device reaches the excellent value of 1 A/W, and it is basically wavelength independent, indicating that incoherent photon-assisted hopping supports charge transport among the few BNCs deposited in the nanogap between the contacts.

A further dramatic change in the transport characteristics occurs for contact gaps of 60 nm (or less), where only one biological nanocrystal is probed. Under this con-

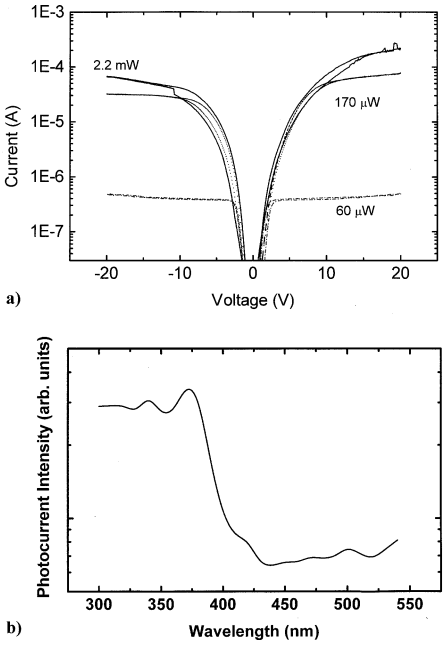

FIGURE 3. (a) Current–voltage curves of the 120-nm gap guanosine device under illumination with increasing light power. The light source used for these experiments was a commercial tungsten lamp. The photoresponse is wavelength-independent. **(b)** Photocurrent spectrum measured as a function of the excitation wavelength for the device with $L = 60$ nm. The photocurrent was measured by biasing the device with −1 V. The photocurrent intensity is on a logarithmic scale.

dition the device becomes asymmetric (FIG. 2c) and strongly rectifying, with currents on the order of a few μA for positive bias (at 10 V) and nA for negative bias and no hysteresis. In the small-voltage region (below ±0.8 V), a zero conductivity region with a steplike onset for both positive and negative voltages is observed, which could be related to tunneling processes through the potential barrier at the metal–BNC contact region or to some image-force that modifies the barrier height. The device exhibits a clear diode-like characteristic, even though there is no external mechanism inducing polarity. Note that the two contacts are identical, and the structure of electrodes and deposition procedures are exactly the same for the three samples examined in FIGURE 2.

The strong differences observed in the characteristics of the devices depending on the distance between electrodes suggest that different conduction mechanisms concur in the overall charge transport, depending on the relative size of the gap (L) versus the self-assembling length (l). Because the ordered guanosine crystal spontaneously forms on a length scale $l < 100$ nm, we distinguish between the coherent transport phenomena within a single BNC (probed in the case of the 60-nm device), and incoherent transport phenomena (like noncoherent tunneling and phonon- or

photon-assisted hopping) that involve neighboring guanosine BNCs in wider gap contacts. Moreover, the observation of an asymmetric *I-V* characteristic in devices in which a single nanocrystal is probed suggests that an intrinsic directional mechanism—such as a strong dipole—must be formed in the BNC, which must be peculiar to the self-organization of the ribbons.

To examine this possibility and to investigate the electronic structure of the BNC, we have modeled a prototype periodic system made of guanine molecules arranged in isolated and stacked ribbon structures. Our calculations are based on the density functional theory (DFT) in the local density approximation (LDA),[15] taking into account BLYP gradient corrections (GGA) to the exchange-correlation functional,[16,17] and using *ab initio* norm-conserving pseudopotentials[18] (plane-wave expansion up to 50 Ry kinetic-energy cutoff). For the atomic positions within the ribbon, we started from the X-ray data (FIG. 1a)[11] and relaxed the structure through a Car-Parrinello-like scheme,[19] until the forces obtained from the full quantum mechanical electronic structure[20] vanished within an accuracy of 0.05 eV/Å.

The resulting geometry, total charge density isosurface, and dipole moment are shown in FIGURE 4b. The single guanine molecule, with calculated structure in excellent agreement with experiments,[21] is also presented for reference (FIG. 4a). There is a strong charge redistribution toward the O atom. From the charge density of the finite systems, we directly calculate the dipole moments. As expected,[22] we find for guanine a large value (about 7 D). In the ribbon, the contribution from the molecules cancel in the direction perpendicular to its axis, yielding a finite and large spontaneous dipole moment lying parallel to the ribbon. (The calculated magnitude of the dipole is 14.6 and 32.8 Debye for a ribbon comprising 2 and 4 guanine molecules, respectively.)

To calculate the electronic structure, we have examined single ribbons as well as vertically stacked ribbons with different stacking geometries along the *z* direction. (Note that the stability of the real stacking will be affected by the sugar molecules and the alkyl chains, not included in the present calculation.) In all cases, the model crystals with relaxed geometries are found to have DFT-GGA band gaps of the order of 3 eV (usually greatly underestimated[15]). The corresponding energy bands along the direction of the ribbon always show negligible dispersion, indicating that no delocalized intermolecular states are present that bridge through the hydrogen bonds. The dispersion along the *z* direction perpendicular to the ribbons is of course very sensitive to the geometrical stacking that controls the π-π interactions. In the "optimal" stacking geometry, that is, with perfectly eclipsed ribbons, the *z* dispersion of the bands derived from the highest occupied molecular orbital (HOMO) and the lowest unoccupied molecular orbital (LUMO) is sizable (FIG. 4c); The calculated effective masses reach the relatively small values of 1.24 m_e for electrons and 1.07 m_e for holes. Their values are, of course, much larger for weaker π–π coupling. From the band-structure calculations, we conclude that the stacked ribbons are reminiscent of very anisotropic wide-gap semiconductors, where a bandlike mechanism for conduction can possibly contribute only along the *z* direction. In the other directions, that is, among the guanine molecules along a ribbon and among adjacent ribbons in the *xy* plane, bandlike conduction is negligible, and a hopping-like mechanism through localized states must dominate.

The theoretical results support the picture of individual BNCs as wide-gap semiconductor nanostructures. This is nicely supported by the observation of a photocur-

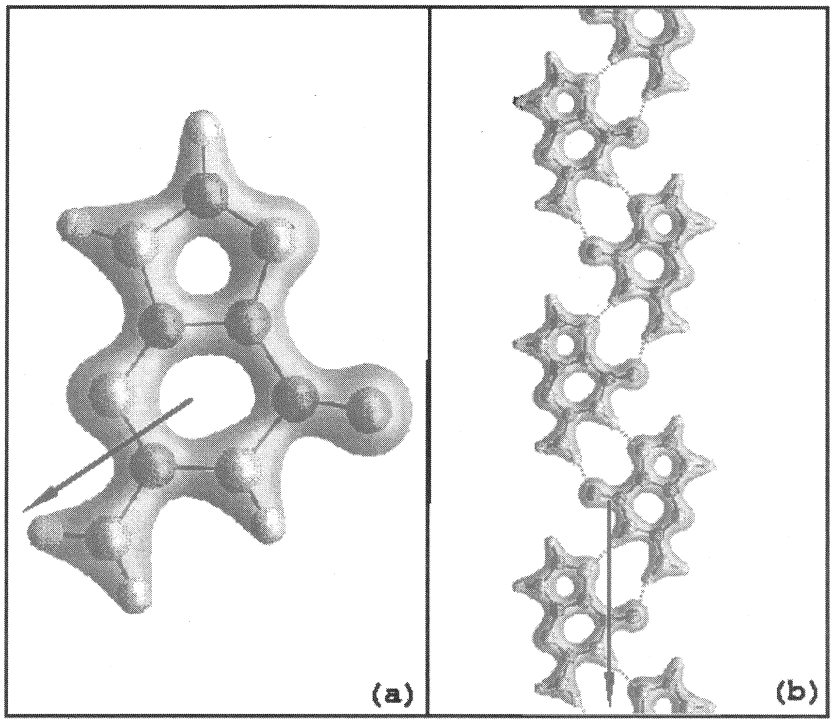

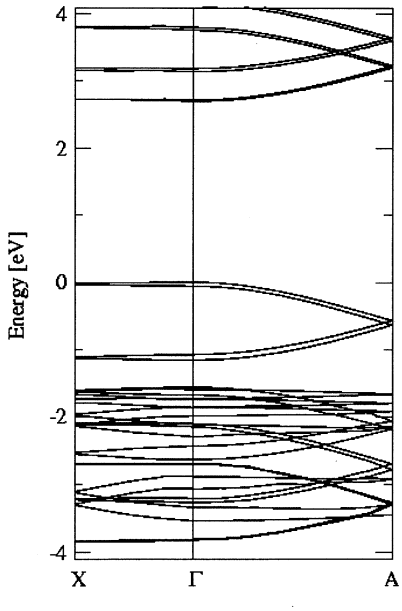

FIGURE 4. Calculated geometry, total charge density isosurface, and dipole moment for **(a)** an isolated guanine molecule and **(b)** a finite hydrogen-bonded guanine ribbon. **(c)** Energy-band dispersion for stacked guanine ribbons in the eclipsed geometry, calculated along the ribbon axis, $\Gamma - X$, and in the z stacking direction, $\Gamma - A$. Here we have taken $A = \pi/2a$, a being the distance between two successive stacked guanine planes.

rent spectrum similar to that of inorganic semiconductors, with a clear absorption onset around 3.5 eV (FIG. 3b), in the device with $L = 60$ nm. Conversely, for length scales larger than the typical size of the self-ordered deoxyguanosine nanocrystal, transport occurs by incoherent tunneling or hopping processes among close nanocrystals, to give overall charge transport across the electrodes, as indeed is inferred from the wavelength-independent photoresponse of the devices with $L > 100$ nm.

The formation of a strong dipole along the parallel deoxyguanosine ribbons forming the nanocrystal is responsible for the clear polarization (asymmetric I–V characteristic) of the devices probing just one BNC. Since the interface between the BNC and the electrode must involve a tunnel barrier, only the few atoms that are closest will participate in the contact; thus the dipole is expected to survive even in the presence of the metal electrodes. In addition, for any orientation of the BNC (except for the improbable case with ribbons running exactly perpendicular to the potential drop), the dipole gives a net component across the nanometer-sized gap, which favors the conduction through the electrodes. Therefore, the overall transport mechanism in the case of a single (or few) BNC connecting the gold electrodes is not dominated by the bandlike transport in the z direction, but rather by the additional charge hopping or tunneling favored by the internal electric field induced by the dipole. The measured device characteristics would be otherwise unobservable, since in the observed two-dimensional ordering (FIG. 1c) the bases in the ribbons are parallel to the xy plane. When many BNCs with random orientations are present between the gold electrodes, the total dipole averages to zero, and the directionality induced by the spontaneous polarization is lost: hence the device characteristic is symmetric.

A striking property of the realized biomolecular device is that it is possible to switch from a rectifying to a MSM diode or a simple nonohmic electronic device behavior by using the same deoxyguanosine layer as active element and choosing the right distance between the electrodes. This is a direct consequence of the self-assembly scale and properties of deoxyguanosine molecules.

In conclusion, we have shown that self-organization of deoxyguanosine molecules, in conjunction with nanolithography, can be used to fabricate a new generation of electronic devices. The most interesting aspect of our results is in the easy fabrication of the device. At the moment the costly step is related to the electrode fabrication by electron-beam lithography (EBL). The achievement of self-organization on a length scale of ~250 nm would allow us to fabricate devices on planar structures made by optical lithography and by using an ink jet printer. The fundamental aspects of our results are relevant as well, in that we show for the first time how the self-organization of DNA bases results in a clear semiconductor behavior that can be exploited in a device. The biological quantum dot investigated here exhibits semiconducting properties and a spontaneous, dipole-induced electric field that are conceptually the same as those occurring in some inorganic quantum dots (see, for example, Fry *et al.*[23]).

ACKNOWLEDGMENTS

We are grateful to V. Fiorentini, R. Blyth, and J. Thompson for useful discussions.

REFERENCES

1. CINGOLANI, R. 2000. Biological software for materials engineering. Nature Biotechnol. **18:** 828–829.
2. WHIGLEY, S.R. *et al.* 2000. Selection of peptides with semiconductor binding specificity for directed nanocrystal assembly. Nature **405:** 665–668.
3. MIRKIN, C.A., R.L. LETSINGER, R.C. MUCIC & J.J. STORHOFF. 1996. A DNA-based method for rationally assembling nanoparticles into macroscopic materials. Nature **382:** 607–609.
4. ALIVISATOS, A.P. *et al*. Nature **382:** 609–611.
5. CHEN, J. *et al*. 2000. Room-temperature negative differential resistance in nanoscale molecular junctions. Appl. Phys. Lett. **77:** 1224–1226; KLEIN, D.L. *et al*. Nature **389:** 699–701.
6. BRAUN, E., Y. EICHEN, U. SIVAN & G. BEN-YOSEPH. 1998. DNA-templated assembly and electrode attachment of a conducting silver wire. Nature **391:** 775–778.
7. OKAHATA, Y., T. KOBAYASHI, K. TANAKA & M. SHIMOMURA. 1998. Anisotropic electric-conductivity in an aligned DNA cast film. J. Am. Chem. Soc. **120:** 6165–6166.
8. FINK, H.W. & C. SCHÖNENBERGER. 1999. Electrical conduction through DNA molecules. Nature **398:** 407–410.
9. PORATH, D., A. BEZRYADIN, S. DE VRIES & C. DEKKER. 2000. Direct measurement of electrical transport through DNA molecules. Nature **403:** 635–638.
10. RINALDI, R. *et al*. 2000. Transport in hybrid electronic devices based on a modified DNA nucleoside (deoxyguanosine). cond-mat/0006402. http://arxiv.org
11. GOTTARELLI, G. *et al*. 1998. The self-assembly of a lipophilic deoxyguanosine derivative and the formation of a liquid-crystalline phase in hydrocarbon. Helv. Chim. Acta **81:** 2078–2092.
12. GOTTARELLI, G. *et al*. The self-assembly of lipophilic guanosine derivatives in solution and on solid surfaces. Chem. Eur. J. **6:** 3242–3248.
13. KIM, N.S., Q.Q. ZHU & P.R. LEBRETON. 1999. Aqueous ionization and electron-donating properties of dinucleotides: sequence-specific electronic effects on DNA alkylation. J. Am. Chem. Soc. **121:** 11516–11530.
14. SZE, S.M., D. COLEMANN JR. & A. LOYA. 1971. Current transport in metal-semiconductor-metal (MSM) structures. Solid-State El. **14:** 1209–1218.
15. DREIZLER, R.M. & E.K.U. GROSS. 1990. Density Functional Theory: An Approach to the Quantum Many-body Problem. Springer-Verlag. Berlin.
16. BECKE, A.D. 1988. Density-functional exchange-energy approximation with correct asymptotic behavior. Phys. Rev. A **38:** 3098–3100.
17. LEE, C., W. YANG & R.C. PARR. 1988. Development of the Colle-Salvetti correlation-energy formula into a functional of the electron density. Phys. Rev. B **37:** 785–789.
18. TROULLIER, N. & J.L. MARTINS. 1991. Efficient pseudopotentials for plane-wave calculations. Phys. Rev. B **43:** 1993–2006.
19. CAR, R. & M. PARRINELLO. 1985. Unified approach for molecular dynamics and density-functional theory. Phys. Rev. Lett. **55:** 2471–2474.
20. BOCKSTEDTE, M., A. KLEY, J. NEUGEBAUER & M. SCHEFFLER. 1997. Density-functional theory calculations for poly-atomic systems—electronic-structure, static and elastic properties and ab-initio molecular-dynamics. Comp. Phys. Commun. **107:** 187–222.
21. SAENGER, W. Principles of Nucleic Acid Structure. Springer-Verlag. New York.
22. HOBZA, P. & J. SPONER. 1999. Structure, energetics, and dynamics of the nucleic acid base pairs: nonempirical ab initio calculations. Chem. Rev. **99:** 3247–3276.
23. FRY, P.W. *et al*. 2000. Inverted electron-hole alignment in InAs-GaAs self-assembled quantum dots. Phys. Rev. Lett. **84:** 733–736.